

# TG/DTA-MS evaluation of methane cracking and coking on doped nickel–zirconia based cermets

Thomaz Augusto Guisard Restivo · Sonia R. H. Mello-Castanho · Jorge Alberto Tenorio

Received: 12 January 2014 / Accepted: 29 June 2014 / Published online: 1 August 2014  
© Akadémiai Kiadó, Budapest, Hungary 2014

**Abstract** Cermet materials based on metallic nickel and cubic zirconia are the key material for applications on solid oxide fuel cells and high temperature water electrolysis. The main advantage is the possibility of direct feeding a hydrocarbon fuel, like methane, or even an alcohol as a source of hydrogen. The reforming reaction on the Ni catalyst surface can produce hydrogen continuously. However, the resulting catalyst poisoning by carbon deposition (coking) imparts their broad application. The work shows the evaluation of coking tolerance of some cermets prepared by mechanical alloying techniques and compares new additives specially chosen in order to avoid coking and increase the catalytic activity. Refractory metal additives besides copper were added to the basic cermet. While copper is a known doping agent that avoids coking, the refractory metals (Mo and W) have a twofold effect: promote sintering at lower temperatures and increase Cu activity due to their mutual immiscibility. Results of TG/DTA-MS analysis demonstrate both refractory metals have increased the coking tolerance as well as the catalytic activity during diluted methane cracking. Molybdenum and tungsten additives are promised regarding the improvement of these cermet materials for high temperature electrochemical devices.

**Keywords** Cermet · SOFC anode · TG–DTA-MS · Carbon poisoning · Catalyst

## Introduction

Cermet materials play an important role nowadays due to their combined properties for functional and structural components, leading to applications such as solid oxide fuel cells and hard tools. The present article explores new concepts in order to obtain distinct properties on nickel-stabilized zirconia (Ni–YSZ), the most employed anode material in solid oxide fuel cell (SOFC) and cathodes for solid oxide electrolysis (SOEC) [1]. The main development efforts aim to allow hydrocarbon and alcohol fuels direct feeding on SOFC devices for hydrogen generation thanks to reforming reactions. However, such fuels induce poisoning on the catalyst (Ni) surface by carbon deposition (coking), the effect being considered the main drawback of solid oxide fuel cells technology [2–5]. Steam reforming processes are said to avoid coking at the expense of reducing the efficiency of the SOFC cell due to fuel dilution with vapor. One alternative solution to the issue considers copper metal doping which is said to avoid carbon deposition, according to some electrochemical, catalytic, kinetic, and quantum density function (DFT) theories [6–8]. A simpler approach is considered in the present work: Cu and C show strong thermodynamic immiscibility and interact repulsively. Therefore, it is believed that the C atoms are repelled by the Cu ones at the catalyst surface, preventing the formation of C–C bonds. By the other side, Cu forms easily an alloy with Ni, decreasing its electrocatalytic function and even the coking tolerance itself [9–12]. These questions were faced up by the same

T. A. G. Restivo (✉) · J. A. Tenorio  
Polytechnic School - USP - Metallurgical and Materials  
Engineering, Av. Prof. Mello Moraes 2463,  
São Paulo 05508-030, Brazil  
e-mail: guisard@dglnet.com.br

T. A. G. Restivo  
UNISO – Universidade de Sorocaba, Sorocaba, SP, Brazil

S. R. H. Mello-Castanho  
IPEN - Nuclear and Energetic Research Institute, Sao Paulo, SP,  
Brazil

immiscibility concept, where a third refractory metal is added to repeal Cu to an unalloyed state.

Mo refractory metal plays a further function: to promote sintering at low temperature. The sintering by activated surface process (SAS) was developed is such a way to take advantage of sacrificial layer coatings on ceramic particles [12–14]. High energy milling (mechanical alloying) techniques were employed to obtain these metallic layers even with opposite metal species, such as the case for Cu and Mo or W. Metallic Mo additive shows useful properties to be used in SAS mode: Mo oxidizes to  $\text{MoO}_3$ , melting at 802 °C, and evaporates at about 1,100 °C. Thus, this sacrificial metallic film, being inert with respect to the ceramic matrix, provides an effective protection to the surfaces after melting and wetting. Afterwards, during the evaporation step, the molten oxide gradually exposes the hidden surfaces with preserved active surfaces, which approach from each other by capillary forces action. The result is a fast sintering at lower temperatures. Our previous paper has demonstrated the sintering is promoted by doping with metallic Cu and further with Mo in addition to Ni–YSZ cermet compacts [13]. The activation energies determined by quasi-isothermal dilatometry methods clearly show lower values when the cermet is doped with these third and fourth metallic components. In the present article, the objective is to evaluate these metallic dopants regarding fuel cracking (methane) and carbon poisoning tolerance.

## Experimental

The starting powders were cubic 8 mols% yttria stabilized zirconia (YSZ),  $13 \text{ m}^2 \text{ g}^{-1}$ , mean particle size  $d(50) = 0.3 \text{ }\mu\text{m}$ , from Tosoh Corp and metallic Ni powder  $d(50) = 3 \text{ }\mu\text{m}$  (Aldrich). The metallic additives  $d(50) = 5 \text{ }\mu\text{m}$  include Cu, W, and Mo. High energy milling was carried out at a 19 Hz shaker mill with vials and  $\phi 5 \text{ mm}$  spheres made from AISI 52100 steel or polymeric vials sheathed by tetragonal zirconia (YTZ) as well as YTZ  $\phi 5$  and 8 mm spheres. Processing milling times were 3–10 h employing balls to powder mass ratios of 10:1 and 20:1. There are low contamination at these condition, approximately 0.3 mass% Fe, Ni e Cr when milled into steel vials. All the prepared compositions include 40 vol% total metal content and 60 vol% of YSZ, were metallic Ni amounts from 20 up to 40 vol%, remaining other metallic additives the rest. Green pellets were pressed at 100 MPa load into  $\phi 7$  and 10 mm dies. Sintering of pellets was performed at different conditions according to the SAS process in a tubular furnace. A dynamic atmosphere of argon ( $150 \text{ mL min}^{-1}$ ) with controlled oxygen partial pressure was obtained by flowing the gas through a thermostated water flask. This procedure assures a humidified argon flow where the water

vapor is weakly decomposed at high temperature providing a small set of oxygen partial pressure during sintering. Milled powders and sintered pellets were analysed by X-ray diffraction (Shimatzu XRD-6000,  $\text{CuK}_\alpha$ , 40 kV) in order to check the validity of the repulsive action between Cu and refractory metals. This means the precipitated Cu peak may be identified beside Ni peaks. The sintered samples analysed by TG/DTA-MS are listed in Table 1 together with the sintering parameters employed. They were chosen among several sintering experiments to find similar densities, e.g., same geometric densities (% TD—theoretical density). Thermal analyser TG/DTA (Setaram Setsys) coupled to a mass spectrometer MS (MKS e-Vison+) was employed under 10 % Ar-diluted  $\text{CH}_4$  and  $\text{O}_2$ , controlled by mass flow system. The specific sensitivity of the MS apparatus is  $1.5 \times 10^{-4} \text{ A mbar}^{-1}$ . Sintered material pieces cut from pellets (masses in Table 1) were charged in cylindrical alumina crucibles and submitted to two  $\text{CH}_4/\text{O}_2$  redox cycles at 800, 650, and 500 °C isotherms. Gas flow sweeps downward to reach the open-top crucible, assuring the reactive gas contacts the porous sample. The recorded TG/DTA-MS curves can be used to follow numbered events of mass loss, energy change, and amount of gas evolved. The Mo bearing sample was further analysed at SEM-FEG/EDS (scanning electron microscope—field emission gun EDS coupled, Jeol model JSM 6701S) .

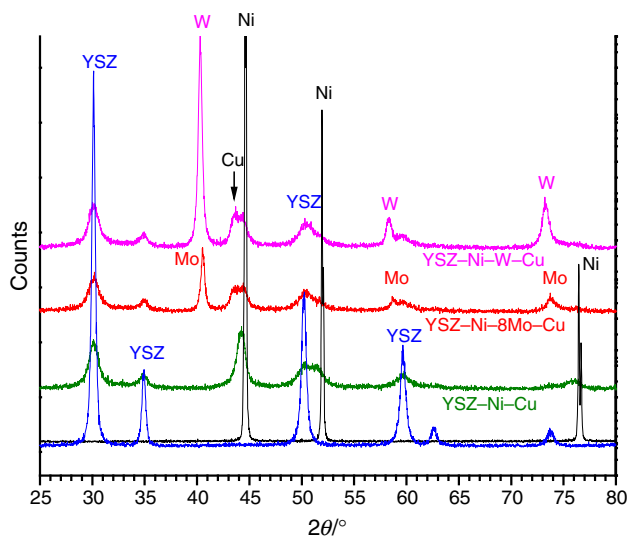
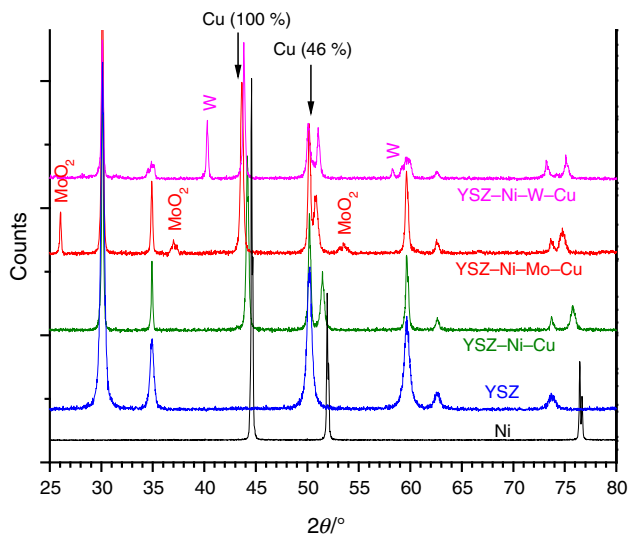
## Results and discussion

Figure 1 shows the X-ray powder diffraction patterns of 3-hours high energy milled sample besides the original Ni and YSZ powders. Peak broadening is evident due to high energy milling action. Microforging events increase the amount of defects like dislocations on Ni powder, while refining the YSZ ceramic powder. The DRX profile for YSZ–Ni–Cu milled powder does not show the main peak related to Cu but only the Ni peak, which indicates the metal forms early an alloy with Ni during powder high energy milling. However, the incorporation of Mo and W additives on powders has preserved Cu peak intensities due to repulsive action exerted by the refractory metals, demonstrating the thermodynamic immiscibility concept is valid. Once Cu is precipitated, it is expected a positive effect on coking tolerance and catalytic activity.

Nevertheless, the precipitation of Cu after sintering the pellet samples is not easily evident as seen in Fig. 2. There are some indications that free Cu is still present in sintered samples containing Mo and W since Ni peaks are strongly shifted and broadened in the direction of Cu-100 % peak. One can note the second Cu peak (46 %) seems to reflect X-ray as compared to YSZ–Ni–Cu one.  $\text{MoO}_2$  is identified for YSZ–Ni–Mo–Cu patterns due to the slightly oxidation

**Table 1** Sintered samples selected for TG/DTA-MS analyses: composition, % of the theoretical density (%TD, geometric measured density), sample masses, and sintering parameters

Sample	Composition/vol%				%TD	Mass/g	Sintering parameters	
	Ni	Cu	Mo	W			Temperature/°C	atmosphere
YSZ-Ni	40	–	–	–	65.8	52.0	1,200	Ar
YSZ-Ni-Cu	28	12	–	–	67.2	68.0	1,200	Ar
YSZ-Ni-8Mo-Cu	20	12	8	–	66.3	70.1	1,200	Ar-p <sub>O2</sub> = 10 <sup>-4</sup> atm
YSZ-Ni-19Mo-Cu	11	10	19	–	65.7	76.2	1,200	Ar-p <sub>O2</sub> = 10 <sup>-4</sup> atm
YSZ-Ni-W-Cu	20	12	–	8	69.3	99.5	1,100	Ar-p <sub>O2</sub> = 1.5 × 10 <sup>-6</sup> atm

**Fig. 1** X-ray diffraction patterns for powders YSZ-Ni-Cu and with refractory metals additives**Fig. 2** X-ray profiles of sintered samples

sintering conditions. The volatile MoO<sub>3</sub> should be evolved during sintering but the sub-oxide remains since it is less volatile.

The simultaneous TG/DTA-MS analysis under redox conditions for YSZ-Ni is shown Fig. 3. During methane flow (10 %) at 800 °C, the reduction is fast followed by a mass loss thanks to some residual NiO in the pellet. The respective DTA peak is endothermic. After reduced, still under methane, the material gains mass, which has been ascribed to carbon deposition on surface (coking). In the sequence, argon is fluxed to purge the reducing gas and O<sub>2</sub> (10 %) is admitted to settle an oxidizing condition. It is interesting to note in the oxidizing O<sub>2</sub> flow period that there is still a mass loss since the previously deposited carbon is oxidized to CO<sub>2</sub>. According to MS simultaneous scanning, methane undergoes cracking to form H<sub>2</sub>, which is detected in the spectrometer, and CO<sub>2</sub> is formed afterwards when flowing O<sub>2</sub>. At lower temperatures, both the reforming and the coking processes are less intense. One further aspect to be noted is the aging of the catalyst after six cycles when heating once more up to 800 °C in the last cycle. It seems to lose the initial efficiency since the hydrogen release is rather small. Hence, YSZ-Ni cermet has low tolerance to catalyst poisoning by coking.

YSZ-Ni-Cu material shows a different behavior (Fig. 4). The mass gain in the reducing step is less intense, meaning there is little carbon deposition, in accordance with lower CO<sub>2</sub> release in oxidative step.

The results are encouraging for YSZ-Ni-8Mo-Cu (Fig. 5) since carbon deposition was not detected as measured by mass gain, even at 800 °C, as well as plenty of hydrogen is released from methane reforming reaction along all the reduction cycles. One important point to mention is the higher stability of hydrogen production during methane flow, as seen by a low slope of H<sub>2</sub> scanning curve. There is even an important amount of hydrogen evolved at 650 °C, demonstrating the catalyst is rather active at this temperature. CO<sub>2</sub> formation is smaller than the previous samples, in spite of some increasing at the

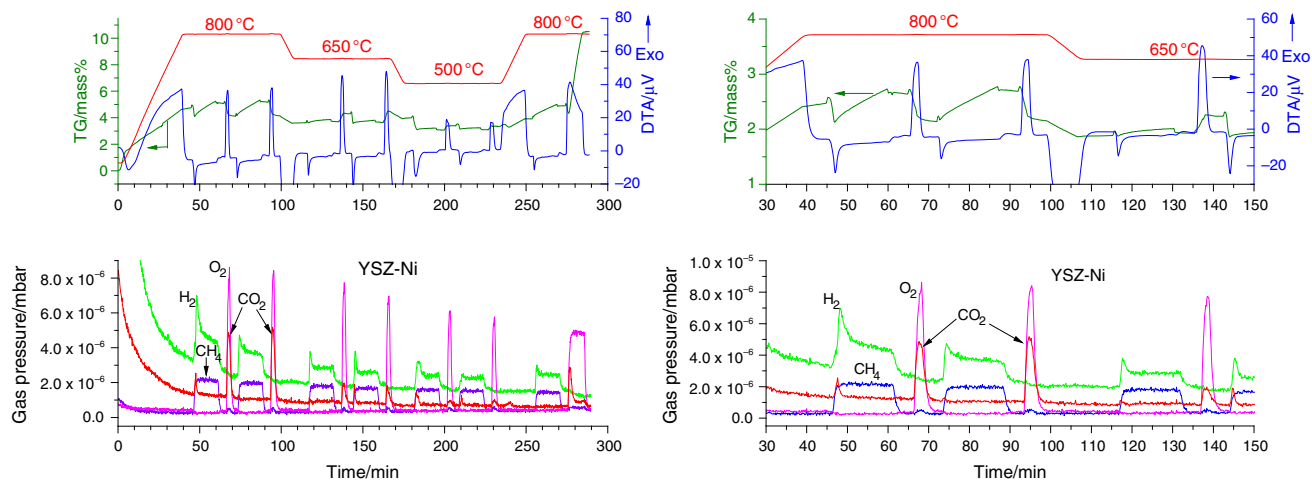


**Fig. 3** TG/DTA-MS analysis of YSZ-Ni under redox cycles; total analysis and 800 °C detail

**Fig. 4** TG/DTA-MS of YSZ-Ni-Cu showing the 800 °C step

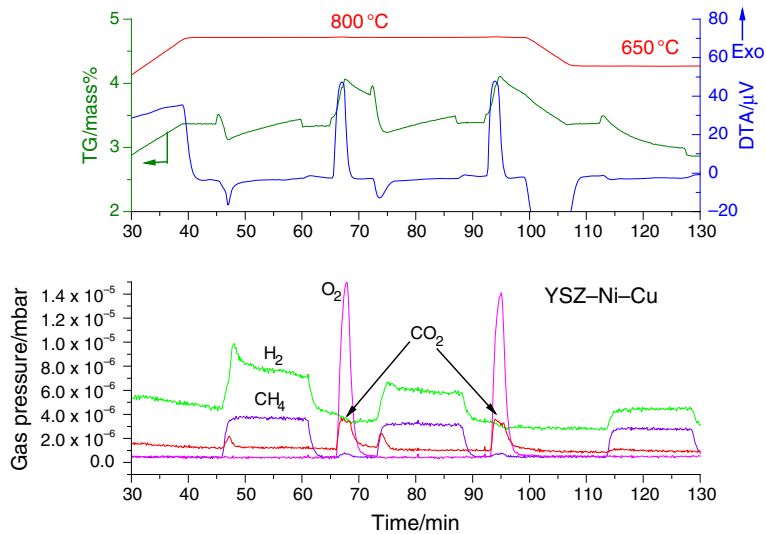
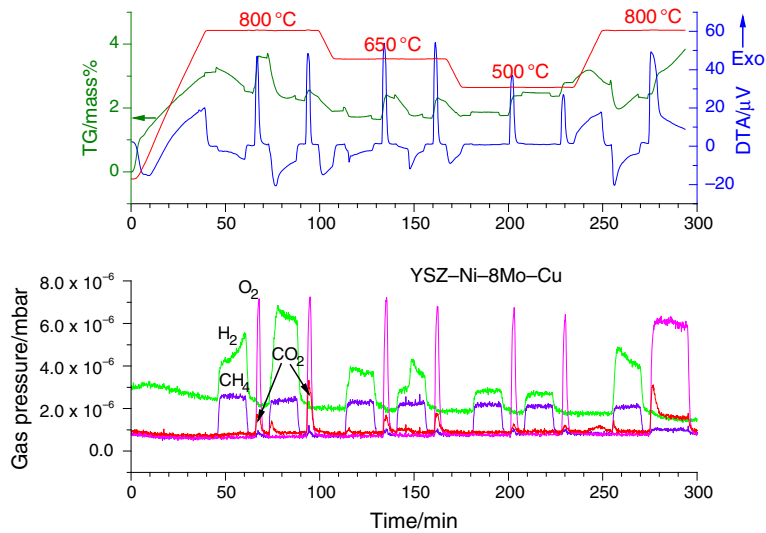


**Fig. 5** TG/DTA-MS of YSZ-Ni-Mo-Cu under redox cycles



second cycle. Moreover, the catalyst remains active at the last 800 °C cycle.

Due to its high solubility in Ni, Mo can form an alloy during high energy milling, sintering, or at 800 °C

isotherm. It is believed the alloyed Mo would force Cu to precipitate at the surface where it would reprecipitate.

Figure 6 compiles the MS signals of H<sub>2</sub> and CO<sub>2</sub> release for different samples, whose measurement curves were normalized by unit mass of sample. Since the sample densities are similar, the same is expected from their pore structure, even though the surface area should be small after sintering. Therefore, a comparison is allowed in unit mass basis. The results show the hydrogen release is higher in samples doped with refractory metals, but not so far from the YSZ-Ni-Cu case. In addition to YSZ-Ni-8Mo-Cu sample, it can be seen the W bearing material is also a good candidate owing to a stable and intense H<sub>2</sub> evolved flow from reformed methane. The hydrogen release from CH<sub>4</sub> cracking expands a longer time to increase to a maximum at the second methane cycle, suggesting the catalyst has undergone an activation sequence. It should be remarked that this kind of phenomena is affected by the original oxidation state of the pellet pore surfaces. Another Mo bearing sample with higher content was also analysed, where the amount of Mo reaches 19 vol%, greater than Ni. In these conditions, the Mo thermodynamic activity in the

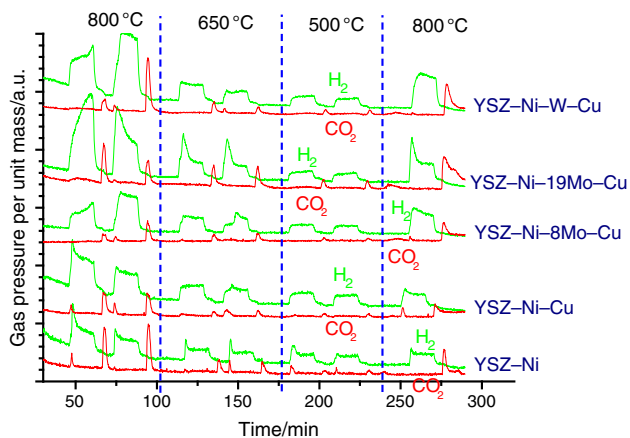


**Fig. 6** Comparison between the cermet materials on releasing gases by unit mass by MS

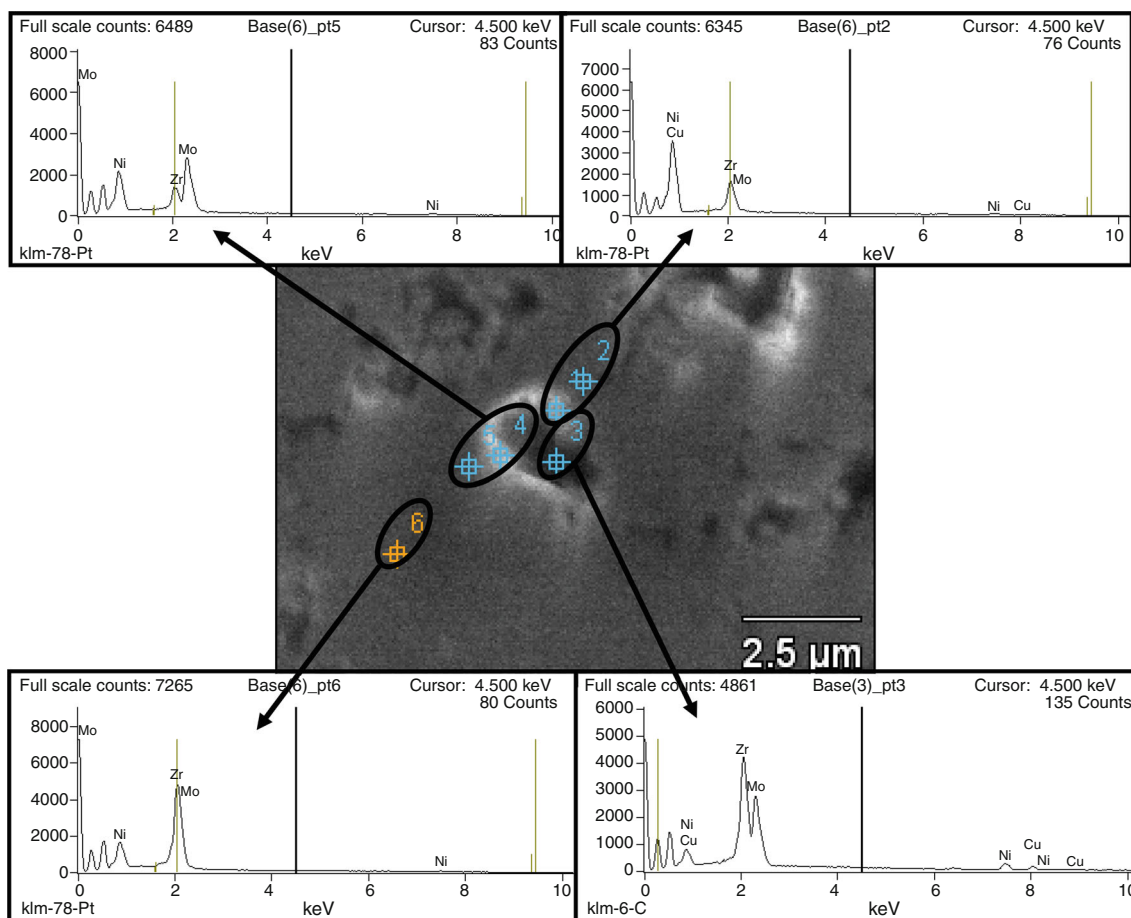


**Fig. 7** SEM-FEG EDS punctual analysis near the pore; sintered YSZ-Ni-Mo-Cu

alloy is unitary and does not admit any dissolved Cu due to repulsive interactions. The respective curves for H<sub>2</sub> and CO<sub>2</sub> show a promised first methane cycle but a catalyst activity degradation in the following cycles. This result suggests the high Mo/low Ni content is not advantageous for the reforming activity of the catalyst. Actually, reforming of methane takes place at Ni sites, as reported for Ni–Mo<sub>2</sub>C catalyst TPR evaluations of CH<sub>4</sub> dissociation [15], which requires higher Ni content. Molybdenum carbide is likely to form in the experiment conditions which could also increase the coking tolerance in addition to Cu repulsing effect on carbon atoms. York has concluded that Mo and W carbides avoid the deactivation of Ni supported catalyst, being WC the most effective [16]. According to this article, the carbide sites form closely to active Ni sites and provoke the decomposition of CO<sub>2</sub>, providing more surface oxygen to oxidizes the deposited carbon on Ni.

The synergetic effect of Mo doping on Ni in increasing the methane cracking activity has been explained by increasing the electron density of Ni due transferred electrons from MoOx species or Mo atoms [17, 18]. Electron pairs donation between Ni and Mo can also lead to formation of stable intermetallic compounds with suitable electronic configuration to provide adherence and transference of H<sup>+</sup> ions, therefore, promoting H<sub>2</sub> evolution from methane. Among the very stable intermetallic compounds, NiW<sub>3</sub> and NiMo<sub>3</sub> exhibit *d*-orbitals overlapping and are expected to show high catalytic activities [19]. Basically, the refractory metals induce Ni to form H bounds such as a hydride but with low stability due to internal intermetallic bounds formed with Ni. Thus, the weakening of H bounds over Ni allows hydrogen evolution.

A more detailed investigation of the cermet microstructure indicates the influence of refractory and Cu distribution on the reforming behavior for the as-sintered YSZ–Ni–Mo–Cu cermet in Fig. 7. Mo (points 3 and 4) and Cu (point 3) are precipitated in the vicinity and surface of pores due to their mutual immiscibility. As disclosed in the X-ray profile in Fig. 2, Mo can be also present as MoO<sub>2</sub> oxide. Free Cu is expected to repeal C atoms, avoiding the formation of C–C bonds, and filament growing that leads to catalyst poisoning. In parallel, Mo carbide is likely to form in place of C chains.

## Conclusions

TG/DTA-MS analyses were performed at sintered cermets of YSZ–Ni containing Cu, Mo, and W as bimetallic and multimetallic alloys under redox condition with argon diluted methane and oxygen. The powder samples were processed by high energy milling, while the compacts were sintered by SAS method. The refractory metals were

employed with two functions: to increase the densification on sintering and to repeal Cu to precipitate from Ni–Cu alloy. The results demonstrate Cu alloying is efficient on blocking carbon deposition regarding YSZ–Ni standard cermet. Low content Mo additive can improve the coking tolerance, while the catalytic activity for hydrogen release from methane cracking is slightly increased. W doping is found to further increase hydrogen evolution in the same conditions. The thermodynamic concept of metal immiscibility is proposed in order to explain the superior coking tolerance, while it is suggested both refractory metals doped can have synergetic effects among those metals and Ni. SEM analysis has found rich regions of Cu and Mo in the vicinity of pores, suggesting these metals have repulsive characteristics when alloyed with Ni and may precipitate. The repulsing action of free Cu against C indicates the principles supported in the research are valid to delay the catalyst deactivation by coking. Multimetallic YSZ–Ni cermets containing Cu, Mo, and W are promised materials for SOFC cells and high temperature water electrolysis, as well as for methane cracking processes.

**Acknowledgements** The authors thanks to CNPq for the financial support (process. Nu. 150672/2012-8) and to the research council FAPESP. Special thanks to INPE-LACP for TG/DTA-MS analyses and Electronic Microscopy Lab of IPEN.

## References

1. Laguna-Bercero MA. Recent advances in high temperature electrolysis using solid oxide fuel cells: a review. *J Power Sources*. 2012;203:4–16.
2. He H, Hill JM. Carbon deposition on Ni/YSZ composites exposed to humidified methane. *Appl Catal A*. 2007;317:284–92.
3. Minh NQ. Ceramic fuel cells. *J. Am. Ceramic Soc*. 1993;76(3):563–88.
4. Atkinson A, et al. Advanced anodes for high-temperature fuel cells. *Nat Mater*. 2004;3(1):17–24.
5. Macet J, Novosel B, Marinsek M. Ni–YSZ SOFC anodes—Minimization of carbon deposition. *J Eur Ceram Soc*. 2007;27:487–91.
6. Bolder M, Dittmeyer R. Catalytic modification of conventional SOFC anodes with a view to reducing their activity for direct internal reforming of natural gas. *J Power Sources*. 2006;155:13–22.
7. Nikolla E, Schwank J, Linic S. Promotion of the long-term stability of reforming Ni catalysts by surface alloying. *J Catal*. 2007;250:85–93.
8. Linic S. Development of Sulfur and Carbon tolerant reforming alloy catalysts aided fundamental atomistic insights. Report No. DE2009-953215, NASA STI; 2008. p. 31.
9. Sun C, Stimming U. Recent anode advances in solid oxide fuel cells. *J Power Sources*. 2007;171:247–60.
10. Gross MD, Vohs JM, Gorte RJ. A study of thermal stability and methane tolerance of Cu-based SOFC anodes with electrodeposited Co. *Electrochim Acta*. 2007;52(1):1951–7.
11. Guisard Restivo TA, Mello-Castanho SRH. Cu–Ni–YSZ anodes for solid oxide fuel cell by mechanical alloying processing. *Int J Mater Res*. 2010;101:128–32.

12. Restivo TAG, Mello-Castanho SRH. New integrated cermet powder preparation and consolidation method Ni-ZrO<sub>2</sub> case. *Mater Sci Forum*. 2010;660–661:370–6.
13. Restivo TAG, Mello-Castanho SRH. Sintering studies on Ni–Cu–YSZ SOFC anode cermet processed by mechanical alloying. *J Therm Anal Calorim*. 2009;97:775–80.
14. Guisard Restivo TA, Yamagata C, Mello-Castanho SRH. Direct Processing of Multimetallic Cermet for SOFC Applications. In: *European Fuel Cell Forum 2010, Lucerne, Chap 9*, 9–15.
15. Shi C, et al. Ni-modified Mo<sub>2</sub>C catalysts for methane dry reforming. *Appl Catal A*. 2012;431–432:164–70.
16. York APE, Suhartanto T, Green MLH. Influence of molybdenum and tungsten dopants on nickel catalysts for the dry reforming of methane with carbon dioxide to synthesis gas. *Stud Surf Sci Catal*. 1998;119:777–82.
17. Maluf SS, Assaf EM. Ni catalysts with Mo promoter for methane steam reforming. *Fuel*. 2009;88:1547–53.
18. Paunovic P, et al. Modifications for the improvement of catalyst materials for hydrogen evolution. *J Serb Chem Soc*. 2006;71(2):149–65.
19. Jaksic MM. Advances in electrocatalysis for hydrogen evolution in the light of the Brewer-Engel valence-bond theory. *Int J Hydrog Energy*. 1987;12(11):727–52.